AD 156964

RF Project 682
Technical Report No. 2

TECHNICAL

REPORT

by

THE OHIO STATE UNIVERSITY
RESEARCH FOUNDATION

Columbus 10, Ohio

To: OFFICE OF NAVAL RESEARCH
Navy Department
Washington 25, D. C.
Contract Nonr-495 (11)
Project No. NR 036-006/10-24-55

On: MECHANISM OF STRESS CORROSION OF AUSTENITIC STAINLESS STEELS IN HIGH-TEMPERATURE CHLORIDE WATERS

Submitted by: R. W. Staehle*, F. H. Beck** and M. G. Fontana***
Department of Metallurgical Engineering

Date: April 1958

* Now at the U. S. Navy, Bureau of Ships, Washington D. C.
** Director of Corrosion Laboratory, Engineering Experiment Station, The Ohio State University.
*** Chairman, Department of Metallurgical Engineering, The Ohio State University.

ABSTRACT

Stress-corrosion cracking of austenitic stainless steels was studied under various conditions of stress, chloride concentration, complete immersion of specimens, intermittent wetting and drying, and presence of oxygen. Stress-corrosion cracking will occur at stresses as low as 2,000 psi at 50 ppm NaCl. A three-dimensional analysis of stress-corrosion cracks was made and a mechanism of cracking proposed.

I. INTRODUCTION

The subject of stress-corrosion cracking in austenite stainless steels has aroused much interest because of the extensive application of the alloy, the low concentrations of the chloride ion at which stress-corrosion cracking occurs, and the low stresses at which cracking propagates in the presence of the chloride ion.

The effect of various chloride salts on the stress-corrosion cracking of austenitic stainless steels has been studied extensively be Edeleanu (1). He shows in general that it is the chloride ion itself that is the culprit, the effect of the cation being relegated to affecting only the conditions of relative time and temperature for cracking. It is generally agreed that the presence of oxygen is necessary for chloride stress-corrosion cracking in austenitic stainless steels. Eckel and Williams (2) have proposed a chloride-oxygen relationship in the specific conditions of intermittent wetting and drying and alkaline-phosphate treated chloride waters. As the oxygen increases, less chloride is required for cracking. Conversely, as the chloride increases, less oxygen is required. For example, at 220 ppm of oxygen no cracking occurs with 0.1 ppm chloride but does occur at 1.0 ppm. On the other hand, at about 800 ppm of chloride, cracking occurs unequivocally at 10 ppm oxygen, whereas none occurs below 0.1 ppm.

The actual role of the chloride ion in stress corrosion cracking does not seem to be well understood. Numerous studies have shown its relationship to pitting (2, 3, 4, 5). It appears that the chloride ion is adsorbed on ferrous surfaces (6) in preference to oxygen, and through the mechanism of continuous film breakdown and repair thus forms local anodic areas which lead to pitting.

The lowest stress at which stress-corrosion cracking of austenitic stainless steels will crack in the presence of chlorides is apparently affected by the anion, temperature and the physical nature of the medium which, in turn, control the chloride to oxygen ratio present at the cracking site. Some authors indicate that the minimum stresses required for cracking are on the order of yield (7, 8), while other investigators indicate that stresses as low as 3,000 to 10,000 psi (9, 2) will produce cracking. Threshold stresses for cracking have been studied in detail by Hoar and Hines (10, 11). They indicate that in boiling $MgCl_2$ the threshold stress for cracking in austenitic stainless steel is about 20,000 psi.

The subject of stress corrosion in all of the prominent alloy systems as well as that in austenitic stainless steels has been studied extensively by many investigators and such an extensive survey of these systems is omitted because of space considerations. For a comprehensive literature survey of stress corrosion cracking see reference 13. The purpose of this paper is to discuss the effect of the relative availability of chloride and oxygen and the applied stress on the morphology of stress-corrosion cracks in austenitic stainless steels.

II. PROCEDURE AND APPARATUS

Stress-corrosion cracking tests were conducted in autoclaves constructed of Type 304L stainless steel, as illustrated in Fig. 1. These units have a 550 ml capacity and are heated by electric resistance tapes. Several layers of asbestos wrapping are placed on top of the heating elements to provide insulation. Each unit contains a thermocouple well; the temperature is controlled by the use of thermocouples in conjunction with standard type temperature controllers. Teflon gaskets are used to make all closures and have been satisfactory up to 500°F at a pressure of 680 psi. The autoclaves are carefully washed before each test run to remove residual chlorides. In starting tests, the autoclaves are assembled around the specimens and specimen supports. Opposite tie bolts are tightened simultaneously to ensure even pressure on the Teflon gaskets. Test solutions are placed in the units by means of a funnel passing through the opening provided for the thermocouple well.

Figure 2 shows a specimen and specimen clamp used to apply a stress to the specimen. All parts of the specimen clamp are Type 304 stainless steel. Applied stress at the center of the specimen is determined by deflection as read from the dial gauge (calibrated in 0.0001" units) shown in Fig. 3 according to the following relationship for a beam loaded at the center:

$$S = 12 \frac{Ecy}{\ell^2}$$

where:

S - fiber tensile stress of the specimen at the half length

E - Young's modulus for stainless steel, 29×10^6

c - 1/2 thickness of specimen

y - deflection at center of specimen

ℓ - gauge length over which the deflection is measured

When the deflection corresponding to a selected stress is determined, the specimen is placed in the stressing jig and held against the gauge marks. Figure 3 shows the specimen about to be stressed. To stress the specimen the screw of the specimen clamp is turned the required amount.

After the specimen is stressed, it is placed on a rack as illustrated in Fig. 4. Teflon strips placed on the supports are used to insulate the specimen from any galvanic effect of the rack and the autoclave. After the rack is loaded, the entire unit is placed in an autoclave and is ready for testing. For testing in the water phase, the specimens are suspended, tension side down, on the lower part of the rack. For testing under conditions of intermittent wetting and drying, vapor phase, or vapor condensation, the specimens are suspended, tension side up, at the top of the

rack. As many as three specimens can be placed on any one level. The rack shown in Fig. 4 enables testing to be conducted in the water and vapor phases simultaneously if the autoclave is only partially filled. When the rack is filled, the entire unit is placed in an autoclave as shown in Fig. 5 and is ready for testing.

Because of the nature of the application of load by beam deflection, only cracking in its early stages is observed. After cracking has progressed a short distance, stress relief sets in. The specimens, measuring 3.4 x 1.0 x 0.225 cm, were cut from Type 347 stock having the following composition:

Element	%
C	0.07
Cr	17.15
Ni	10.36
Si	0.61
Mn	1.48
P	0.018
S	0.015
Nb	0.97

All specimens were held at 2,000°F for 1/2-hour and furnace-cooled. Three different surfaces were studied: 1) belt-abraded with 120 grit, 2) pickled six hours in concentrated HCl, and 3) electrolytically polished. The first had residual surface stresses, while the last two did not.

The NaCl concentration of the solution was varied from 50 to 80,000 ppm. In all cases the autoclave was filled with 200 ml of solution. For specific studies on the effect of various gases on the propensity to stress-corrosion cracking, 100% oxygen, hydrogen or nitrogen atmospheres filled the remaining 350 ml. Where these gases are not specifically mentioned, air was the gas in the autoclave.

Tests were run for various lengths of time. Since the cracking for all concentrations and for the various physical conditions appeared to be fully developed after four hours at 400°F, the length of the various tests will not be discussed in detail.

Figure 5 shows that the sides, but not the top, of the autoclaves are insulated. This enables a type of intermittent wetting and drying conditions to be present without manually inverting the autoclaves. In the initial experimental work, this type of intermittent wetting and drying was confused with a saturated vapor phase. Cracking was observed when a specimen was suspended in the vapor phase with the tension side up. However, when a Teflon shield was placed above the specimens, none occurred unless the autoclaves were manually and periodically inverted. Since the cracking appeared to be the same whether the condensation from the top fell on the specimen or when the autoclaves were manually inverted,

it was decided to use the vapor condensation condition for producing cracks. Such a technique undoubtedly produces an uncertainty in the chloride composition actually present on the specimen, but the uncertainty is probably no greater than that involved in the manual inversion of the autoclaves.

Surfaces were prepared for photomicrographs by abrading with 240-, 500-, and 600-grit wet-back paper and subsequently by polishing with No. 2 and No. 3 alumina. An electrolytic etch in oxalic acid was used to define grain boundaries, inclusions and cracks.

In cases where it was desirable to show a crack in three dimensions, a special technique was used. The specimen was first mounted in thermo-setting plastic, polished and etched. The crack was first photographed on the tension surface of the specimen. The specimen was then polished at right angles to the tension surface to show the depth and character of the crack. Sections of the crack were polished at incremental distances along the crack as shown in Fig. 6. In some cases, sections of 0.001" thick were removed at a time. To give a three-dimensional effect, the depth of cracking was plotted as a function of the surface length of the crack.

III. RESULTS

A. VAPOR CONDENSATION CONDITION

The experimental data from the vapor condensation conditions are summarized in Table I. The solution concentrations given in this table indicate only the initial composition of the solution. Chemical analyses for chloride following a test showed that the solution composition was unchanged during the test. The composition of any solution actually on the specimen is not known, although the chloride on the surface of the specimen probably becomes more concentrated than that of the solution. The results shown in Table I indicate that chlorides must be present for the stres-corrosion cracking to occur and that the cracking will occur at least as low as 50 ppm NaCl in the solution and at stresses as low as 2,000 psi on pickled specimens free from residual stresses due to abrading. At low chloride levels, the applied stress did not influence the cracking (i.e., at 50 ppm the specimens stressed at 40,000 psi showed no more tendency to crack than those stressed at 2,000 psi).

The presence of 100% oxygen at 50 ppm definitely increases the propensity to cracking. Whereas only half of the specimens cracked at 50 ppm in the presence of air, all of them cracked when the atmosphere was 100% oxygen. It also appears that specimens with abraded or pickled surfaces were equally susceptible to cracking at comparable chloride levels, while the electropolished specimens did not crack until 200 ppm NaCl was reached. These results indicate that a smooth surface may present a more difficult environment upon which to nucleate a pit or crack.

The presence of oxygen was shown to be necessary for cracking to occur. Comparing the results at 875 ppm in Table I, the complete exclusion of oxygen by either nitrogen or hydrogen stops cracking, while the presence of 100% oxygen as described above increases the propensity to cracking.

The residual surface stresses on the abraded specimens produced cracking patterns much different from those on the stress-free pickled specimens. On the pickled surfaces, the cracks were perpendicular to the lengthwise axis of the specimen and occurred at the region of highest applied stress (i.e., at the half length). The cracking on the abraded specimens was irregular with respect to the region of highest stress. Cracks occurred as frequently near the end of the specimens as near the center or region of highest stress. Such a crack distribution probably results from disarrayed surface stresses induced by abrading. In some cases, as shown in Table I, cracking on the abraded surfaces occurred in the absence of applied stress. Several of these cracks are shown in Fig. 7. An entire three-dimensional description of a crack from a pickled specimen is shown in Figs. 8, 9, and 10. The surface of the crack on the tension side of the specimen is shown in Fig. 8, the penetration in Fig. 9, and the plot of the penetrations or the third dimension in Fig. 10. This crack is typical of those occurring at 2,000 psi.

A cracking pattern of a crack in an abraded surface is shown in Fig. 11. This crack occurred at an applied stress of 3,000 psi. Two factors distinguish the cracking on the abraded from the pickled specimens. First, the cracking on the abraded specimens was only half as deep as that on pickled specimens. Secondly, there is usually a number of smaller cracks in the vicinity of the larger crack, probably resulting from a complex interaction of residual stresses.

In addition to the characteristic cracking patterns described in Figs. 8, 9, 10, and 11, some rather unusual patterns occurred on the pickled specimens. Figure 12 shows what appears to be a "circular" crack. The direction of subsurface cracking is not perpendicular to the tension surface, probably because of the complex stresses produced by the initial cracking pattern.

Throughout the photomicrographs there are a large number of pearl-like inclusions, the exact composition of which is not known but is probably a nitride. These inclusions have been observed to arrest the progress of a crack as shown in Fig. 13A and have no retarding effect on crack movement as shown in Figs. 13B and 13C. Figure 13B shows that the inclusion has actually been by-passed by the crack, whereas the inclusion in Fig. 13C exhibits an apparent brittle fracture.

B. WATER PHASE

Table II summarizes the results of the water-phase testing. These results present a much different picture of stresses and chloride concentrations. Instead of cracking at the low concentrations, no cracking is

observed until 20,000 ppm is reached, and no cracking is observed at concentrations greater than 25,000 ppm. The stresses required for cracking, 30,000 psi or above, are much higher than the mere 2,000 psi required in the vapor condensation conditions.

Although the susceptibility to cracking does not change with surface preparation, the nature of the cracking changes markedly. The cracking of the pickled surfaces is shown in Figs. 14 and 15; the cracking of the abraded surfaces is shown in Figs. 16 and 17. Note the single crack when there are no complex surface stresses. The character of the cracks as they progress through the metal should be compared with the cracks occurring in the vapor condensation condition. It appears that there was much more electrochemical attack associated with the cracking in the water phase.

C. CRACK PROPAGATION

A detailed study of the crack propagation kinetics was not possible with the equipment employed in this study; however, a cursory study was made for purposes of comparison with available data. By holding the autoclaves at 400°F for 0.5, 1.0, 2.0, 2.5, 3.0, and 6.0 hours and using stress levels of 3,000 and 7,000 psi, it was determined that cracks begin propagating in about 0.5 hour and are fully developed between 2.0 and 6.0 hours. Since the maximum crack depth observed was 0.4 mm, the rate of cracking probably lies in the range from 0.2 mm/hr to 0.067 mm/hr. These figures are in approximate agreement with those of Hoar and Hines (10), who suggest that cracks in austenitic stainless steels propagate at the rate of 1-4 mm/hr in a boiling $MgCl_2$ solution under stresses on the order of yield. Since actual brittle fractures occur at much higher velocities, it might be concluded that the progress of the stress corrosion cracks is dependent upon an electrochemical action for movement, while the stress plays the role of activating or helping to initiate the cracking.

IV. DISCUSSION OF RESULTS

The annealed ultimate tensile strength of the 300 series of stainless steels is approximately 85,000 psi; the yield strength is approximately 35,000 psi at 0.2% offset; and the threshold stress for stress-corrosion cracking in the vapor condensation condition may be lower than 2,000 psi. The burden of this discussion is to suggest explanations for such insidious behavior.

A. CRACK INITIATION

The chloride concentration and stresses at which cracking occurs in the water phase and vapor condensation conditions give a clue to the mechanism of crack initiation. It appears that the mechanism of crack initiation is related to the available oxygen, specific concentrations of the chloride ion, and the stress level. The significance of these

factors lies in the comparison between the conditions leading to cracking in the water phase and vapor condensation conditions. In the vapor condensation condition there is a ready availability of oxygen, but the chloride level in the water below the specimen was much lower than that required for cracking in the water phase. It is suspected that the chloride achieved high local concentrations through a constant cycle of drops of solution falling on the specimens and the subsequent evaporation. This high local chloride concentration together with the abundant oxygen in the air produced a type of pitting or initial attack that lead to the cracking at the unusually low stresses.

In contrast to the cracking at the low chloride concentrations in the vapor phase, there is no cracking at the low chloride concentrations of the water phase. Cracking in the water phase did not proceed until there was sufficient chloride concentration to produce cracking with the relatively low oxygen concentration in the water. The disparity in the threshold stresses between the vapor condensation and the water phase is probably accounted for by the type of pit formed under the conditions of chloride and oxygen concentrations present. Whereas the pit formed in the vapor condensation conditions would have a high depth-to-radius ratio, the same ratio for the pitting in the water phase would be much lower and, hence, require a higher applied stress to propagate. There is also no obvious reason for the resultant stresses to be extremely high because the cracking does not necessarily propagate by mechanical fracture. It can just as easily propagate by a predominantly electrochemical mechanism with the applied stress supplying just enough strain energy or plastic deformation to exceed the energy requirements for crack propagation. The variance in the types of pitting in the two conditions can be seen in Figs. 8 and 16. The pits on the pickled specimens in the vapor condensation conditions have a small surface diameter (although no data are available on the actual pit configuration just prior to crack initiation), and the pits in the water phase have a much larger surface diameter, in some cases by a factor of about 20. These observations tend to confirm the above hypothesis.

This explanation for the apparently dissimilar conditions that lead to cracking would not seem to account for the absence of cracking at the higher chloride concentrations in the water phase. The only possible explanation would be that, with the higher chloride levels, there is a decrease in the solubility of oxygen, which has been reported by Asselin and Rohrman (12) for another temperature range.

A verification of the saucer-like depressions occurring in specimens immersed in solution has been made by Hoar and Hines [ ], who have observed that, on wire specimens in the aqueous $MgCl_2$, the pitting actually takes the form of saucer-like depressions.

There is no obvious answer to the question of how the sites for crack initiation are chosen. The most likely mechanism involves the continuous breakdown and repair of the surface film. The film breaks down

and the chloride ions adsorb on the surface before the oxygen and lead to the formation of an anodic area. This tendency for the chloride ion to displace the oxygen has been verified by Hackerman and Stephens (6).

Considering next the macro scale, the cracking on the stress-free pickled surfaces always occurs at the half length. This happens in spite of the fact that, when a stress at that point might be 15,000 psi, the stress near the end might be 1,000 to 2,000 psi which, on other specimens stressed to this level at the center, crack at the center. In other words, the cracking always occurs at the center of the specimen in the region of the highest stress. This is not easily understood on the basis of stress relief of a beam-loaded specimen since the cracking might initiate at any location when the specimens are highly stressed. It is probable that the galvanic effect of a highly stressed region can accentuate the pitting tendency at the center of the specimen.

The cracking patterns of the abraded specimens apparently confuse the above hypotheses. The cracking frequently occurs at any location on the specimen, and the prevalence of pitting is not so obvious, although pits were apparent on many of the cracks. Since there is not positive control on the cracking of the abraded specimens, as in the case with the stress-free surfaces, no positive hypothesis can be advanced on the basis of the cracking patterns. The presence of the residual stresses probably obscures the mechanisms which are more readily apparent on the stress free surface.

B. CRACK PROPAGATION

For the purposes of the discussion on crack propagation only, the cracking on the stress-free pickled surfaces will be considered since the cracking patterns on the abraded surfaces have been disrupted by the presence of residual stresses and the interpretation of the cracks would be clouded with extraneous factors.

Figures 8, 9, and 10 will be the basis for the proposed mechanism of stress-corrosion crack propagation. The most significant single fact in the interpretation of crack propagation is that only between 1,000 and 2,000 psi are required for cracks to propagate under conditions of vapor condensation. Cracking at the higher stresses in the water phase seems more credible since the stress required for cracking is only a factor of 3-4 less than ultimate strength rather than a factor of about 50 in the case of the vapor condensation.

On the basis of Fig. 8, cracking in the vapor condensation condition may be divided into stages. First is the pitting stage. Note the large pit in the approximate center of the crack. This pit coincides with a relatively large circle of reaction products observed on the specimen when it was removed from the autoclave. The next stage is actually the first stage of crack propagation. The character of the center one-third of the crack is basically different from the rest of the crack. At this

point the crack is not sufficiently deep to give an effective stress raiser. The second stage of crack propagation can be interpreted as a series of continuous bursts of crack progress. The crack has achieved a critical depth-to-root radius ratio and there is less difficulty in maintaining a continued crack movement. If the applied load in this experiment was constant, catastrophic cracking would be the next stage of cracking; however, the stress relief inherent in beam-loaded specimens causes the crack to stop before this stage is reached. This periodic mechanism observed on the surface of the crack is obvious in Fig. 9, which shows the crack as it progresses through the bulk metal.

The same pattern of cracking stages is apparent in the water-phase cracking shown in Figs. 14 and 15. The large pit or depression in the center seems to have been the point for crack initiation. To the right of the crack there appears to be the pattern of abortive branching followed by a more continuous type of crack. In the bulk metal there is again an indication of a periodic progress, but points of change are not so definite. It appears that the actual progress of the crack is obscured by a much more extensive electrochemical attack than was observed in the vapor condensation conditions. The cracking in the water phase seems to be much more ragged, probably resulting from a more abundant supply of chloride ions in that water phase than in the vapor condensation condition. In fact, the ragged appearance resulting from more extensive electrochemical attack can probably be correlated with the large surface area of the pits.

A tentative conclusion based on the mechanism of crack propagation would be that the cracking is primarily electrochemical, with the stress playing the role of film breaker or, at the most, flowing the metal at the base of the crack which would lead to a high strain energy. On the basis of the low stress and the crack velocity connected with the cracking in the vapor condensation conditions, a type of periodic electrochemical mechanism is much more credible than one in which the stress actually contributes to the crack progress by a fracture mechanism.

V. SUMMARY AND CONCLUSIONS

1. Type 347 stainless steels are susceptible to stress corrosion cracking in the presence of 400°F chloride-containing waters when exposed to vapor condensation conditions. The threshold stress applied for this condition is lower than 2,000 psi and chloride concentrations as low as 50 ppm in the water will produce cracking. Increasing the oxygen concentration from that in air to 100% increases the probability of cracking at low chloride concentrations, while the presence of 100% hydrogen or nitrogen above the solution eliminates cracking.

2. Type 347 is susceptible to stress-corrosion cracking under highly specific conditions when immersed in chloride solutions at 400°F. The solution concentration range of susceptibility is 20,000 to 25,000 ppm NaCl and the stresses must exceed 30,000 psi.

3. Type 347 does not crack in a saturated vapor phase (no condensation) over an 875 ppm NaCl solution at 400°F.

4. Cracking progresses periodically. After the initial pit forms, the crack progresses in short abortive branchings. In the second stage of cracking, the cracks move in longer bursts of 2-10 grains in length. The onset of this stage is probably controlled by a certain stable crack size reached in the first stage. The third stage would be catastrophic cracking if the specimen were under constant load instead of being beam-loaded. (AUTHOR)

5. On the basis of the cracking at the low stresses, it is proposed that the actual crack movement results from electrochemical action with the stress serving to provide a local region of highly stressed metal at the base of the crack. This highly stressed metal provides a local anodic area for preferential electrochemical dissolution.

VI. ACKNOWLEDGEMENT

The support of this investigation by the Office of Naval Research is gratefully acknowledged. This paper is based on a thesis (13) presented in partial fulfillment of the degree, Master of Science, at The Ohio State University.

VII. LITERATURE CITED

1. C. Edeleanu, "Transgranular Stress Corrosion in Chromium-Nickel Stainless Steels," J. Iron and Steel Inst., 173 (1953), 140.

2. W. Lee Williams, "Chloride and Caustic Stress Corrosion of Austenitic Stainless Steel in Hot Water and Steam," presented, Symposium on Basic and Applied Science in the Navy, March 19-20, 1957.

3. M. A. Streicher, "Pitting Corrosion of 18-8," J. Electro-chem. Soc., 103 (July 1956), 375.

4. H. H. Uhlig, "Adsorbed and Reaction-Product Films on Metals," J. Electrochem. Soc., 97 (1950), 215-c.

5. H. H. Uhlig, J. Wulff, Trans. AIME, 135 (1939), 494.

6. Norman Hackerman, Sarah J. Stephens, "The Adsorption of Sulfate Ions from Aqueous Solution by Iron Surfaces," J. Phys. Chem., 58 (1954), 904.

7. Russell Franks, W. O. Bender, Charles M. Brown, "The Susceptibility of Austenitic Stainless Steels to Stress Corrosion Cracking," Symposium on Stress Corrosion Cracking of Metals ASTM-AIME (1944).

8. T. P. Hoar, J. G. Hines, "The Stress Corrosion Cracking of Austenitic Stainless Steels, II, Fully Softened Strain Hardened and Refrigerated Material," J. Iron and Steel Inst., 184 (October 1956), 166.

9. M. A. Scheil, "Some Observations of Stress Corrosion Cracking in Austenitic Stainless Alloys," Symposium on Stress Corrosion Cracking of Metals ASTM-AIME (1944), p. 395.

10. T. P. Hoar, J. G. Hines, "The Stress Corrosion Cracking of Austenitic Stainless Steels," J. Iron and Steel Inst., 182 (1956), 124.

11. U. R. Evans, "Stress Corrosion: Its Relation to Other Types of Corrosion," Corrosion, 7 (1951), 238.

12. F. J. Asselin, F. A. Rohrman, "Corrosion of Copper by Sodium Halide Solutions," Ind. Eng. Chem., 32 (1940), 1015.

13. R. W. Staehle, "A Study of the Mechanism of Stress Corrosion Cracking of Austenitic Stainless Steels in High Temperature Chloride Waters." Thesis. The Ohio State University (1957).

TABLE I

RESULTS OF TESTS CONDUCTED IN THE PRESENCE OF VAPOR CONDENSATION CONDITIONS IN AUTOCLAVES HEATED TO 400°F

NaCl (ppm)[a]	Applied Stress (1000 psi)	Surface	Cracking
Distilled Water	5, 15, 40	A	NO
50	2, 5, 10	P	susc[c]
50 and O_2	5, 10	P	yes
100	5, 15, 40	A	yes
100	5, 10	P	susc
100	5, 10	E	no
100 and O_2	5, 10	P	yes
150	5, 10	P	susc
150 and O_2	5, 10	P	yes
200	5, 10	E	susc
875	0[d], 2, 5, 15, 40	A	yes
875	1, 2, 5, 15, 40	P	yes
875	3, 10	E	susc
875 and O_2	5, 15, 40	A	yes
875 and N_2	5, 15, 40	A	no
875 and H_2	5, 15, 30	P	no
5,000	5, 15, 40	A	yes
10,000	0, 2, 4	A	yes
10,000	5, 15, 40	P	yes
20,000	3, 5, 15, 40	A	yes
20,000	3, 5, 15, 40	P	yes
40,000	5, 15, 40	A	yes
80,000	5, 15, 40	A	yes

a Where a specific gas is designated after the chloride concentration the remaining 350 ml of the autoclave is filled with the particular gas. Otherwise the gas atmosphere is air.

b A - abraded, P - pickled, E - electropolished.

c Cracking occurred in about 50% of the specimens with no preference for stress level.

d The residual stresses due to abrading the specimen were sufficient to cause surface cracking in the absence of applied stress.

TABLE II

RESULTS OF WATER PHASE TESTS CONDUCTED IN AUTOCLAVES HEATED TO 400°F

NaCl (ppm)	Applied Stress (1000 psi)	Surface[a]	Cracking
0	5, 15, 40	P	none
100	5, 15, 40	P	none
875	5, 15, 40	A	none
15,000	20, 35	P	none
		E	none
20,000	20	P	none
		E	none
20,000	40	A	yes
20,000	30	P	yes
20,000	35	P	yes
		E	yes
25,000	35	P	yes
		E	yes
25,000	20	P	none
		E	none
40,000	20, 40	P	none
75,000	20, 35	P	none
80,000	20, 40	P	none

a P - pickled surface; A - abraded surface; E - electropolished surface.

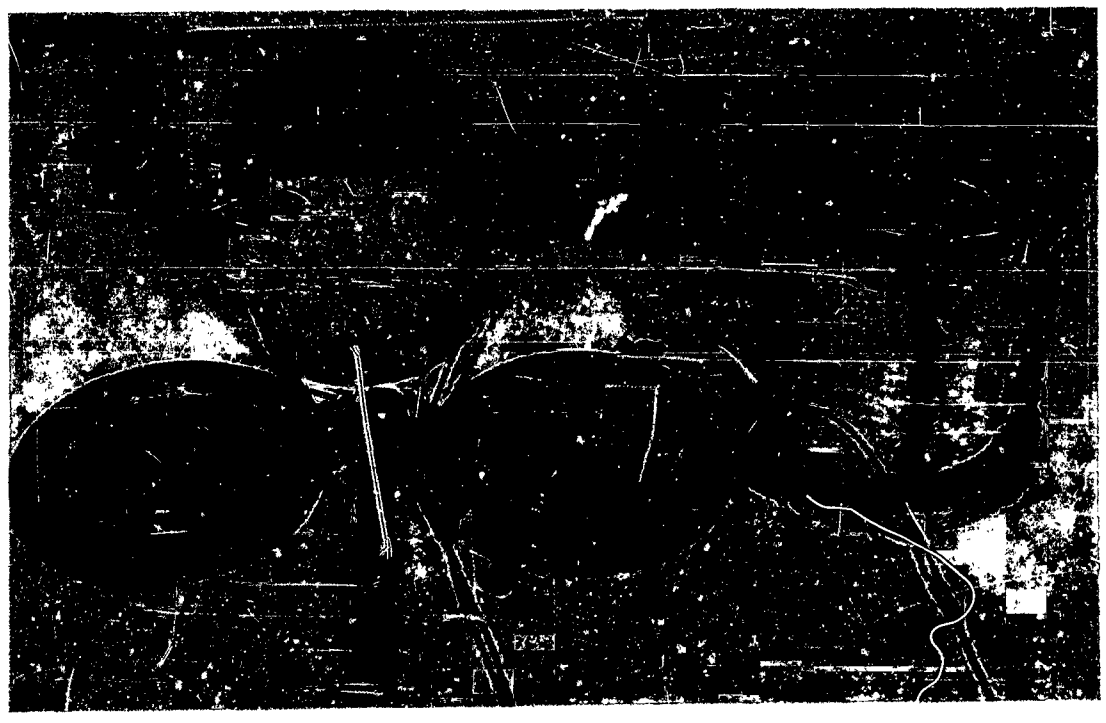

Fig. 1 Auto-laves used in stress corrosion cracking studies

Fig. 2 Exploded and assembled views of stress-corrosion specimen and stressing jig

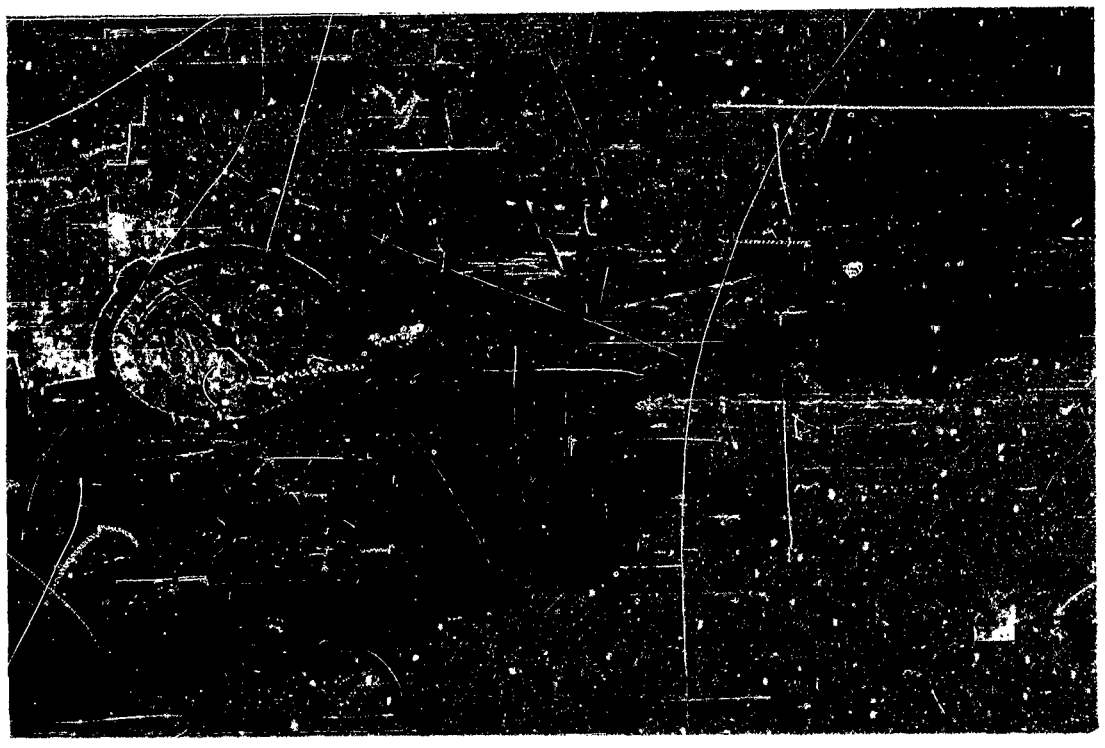

Fig. 3 Specimen being stressed in jig

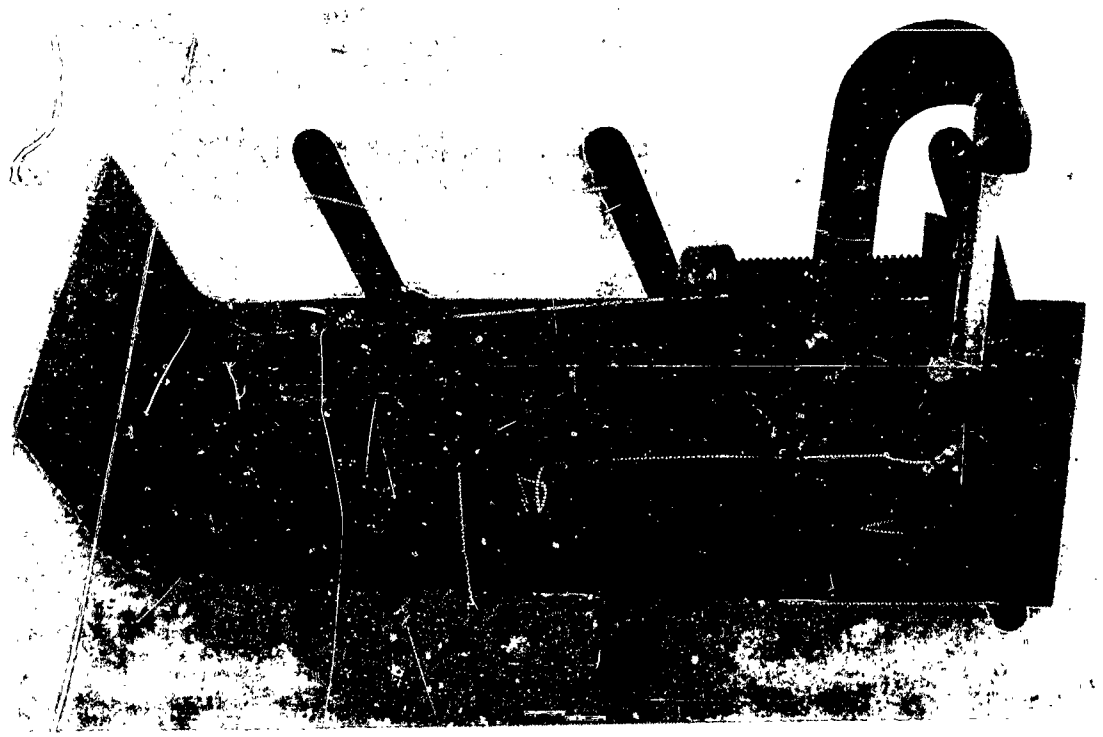

Fig. 4 Specimen support rack

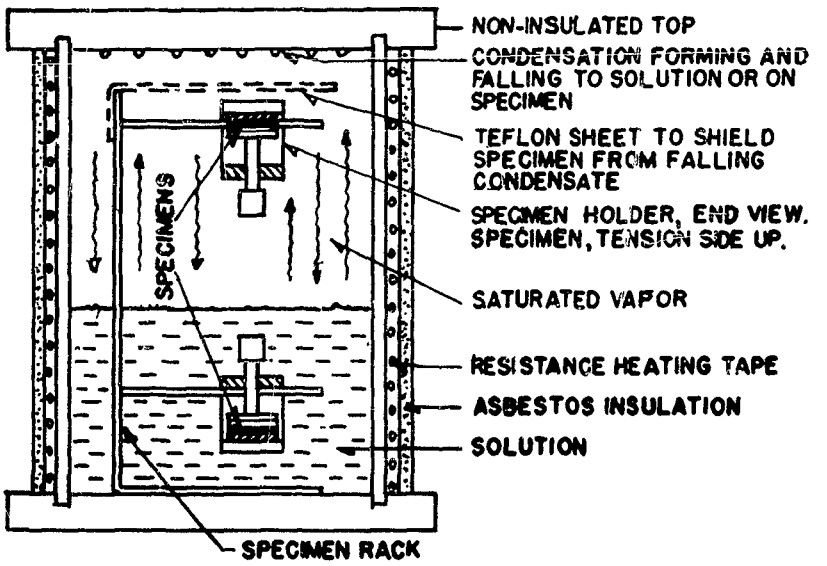

Fig. 5 Cross section of autoclave in operation. Specimens shown in the water phase, vapor condensation (without Teflon shield) and saturated vapor (with Teflon shield) phase.

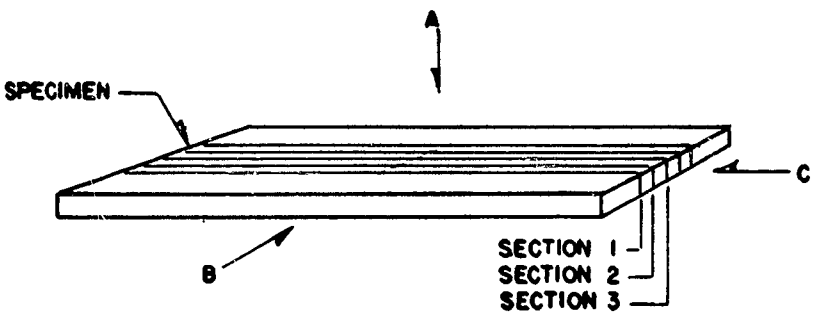

Fig. 6 Schematic of sectioned specimen. The surface of the crack is viewed in Direction "A" and the cross section in Direction "B". A series of photographs from Direction "A" and Direction "B" can describe the crack from Direction "C".

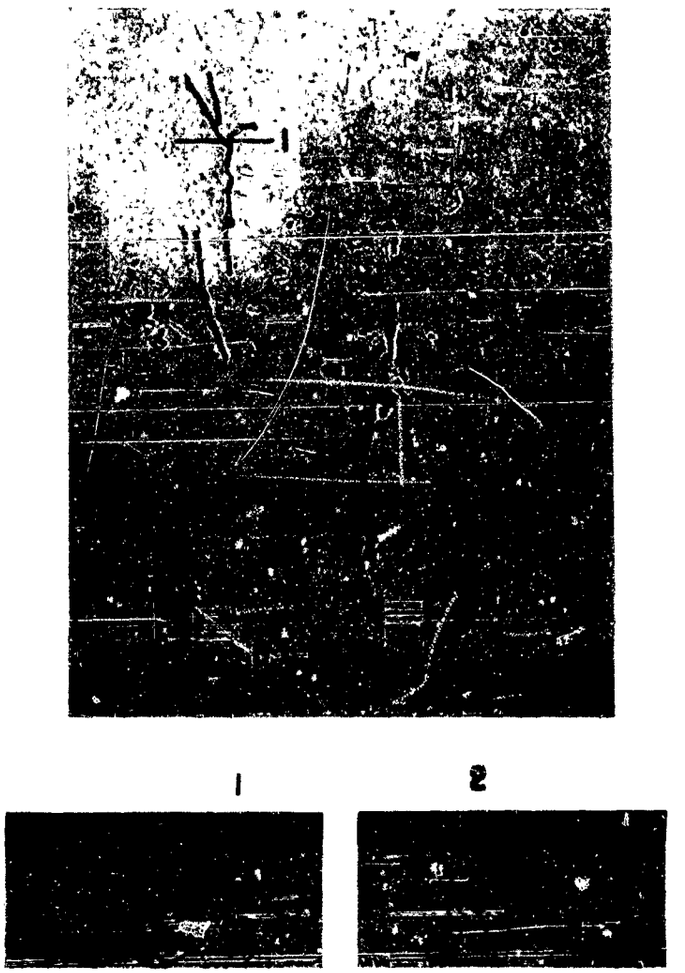

Fig. 7 Surface and cross sectional views of cracking on surface A (see Fig. 6), abraded with 120 belt with no applied stress. Vapor condensation conditions over solution containing 50 ppm chloride. 350x

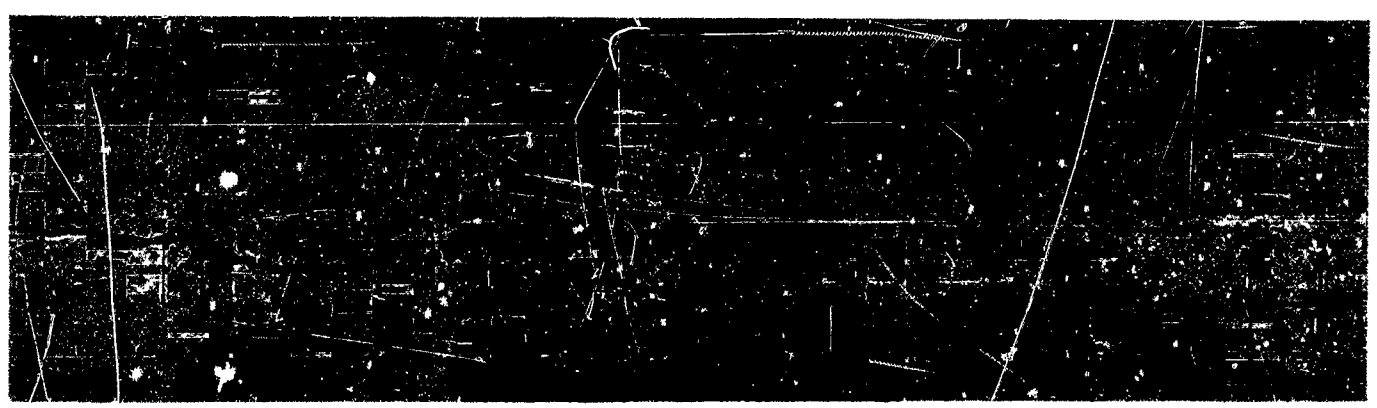

Fig. 8 Surface of typical crack, pickled surface, 400°F, chloride containing waters, vapor condensation conditions. Crack shown etched and unetched. Middle third of crack shows numerous transition points indicating incipient stages of cracking. Remainder of crack shows the transition points more separated. These are encircled and may be either pits or slight direction changes. Numbers refer to cross sections shown in Fig. 9.

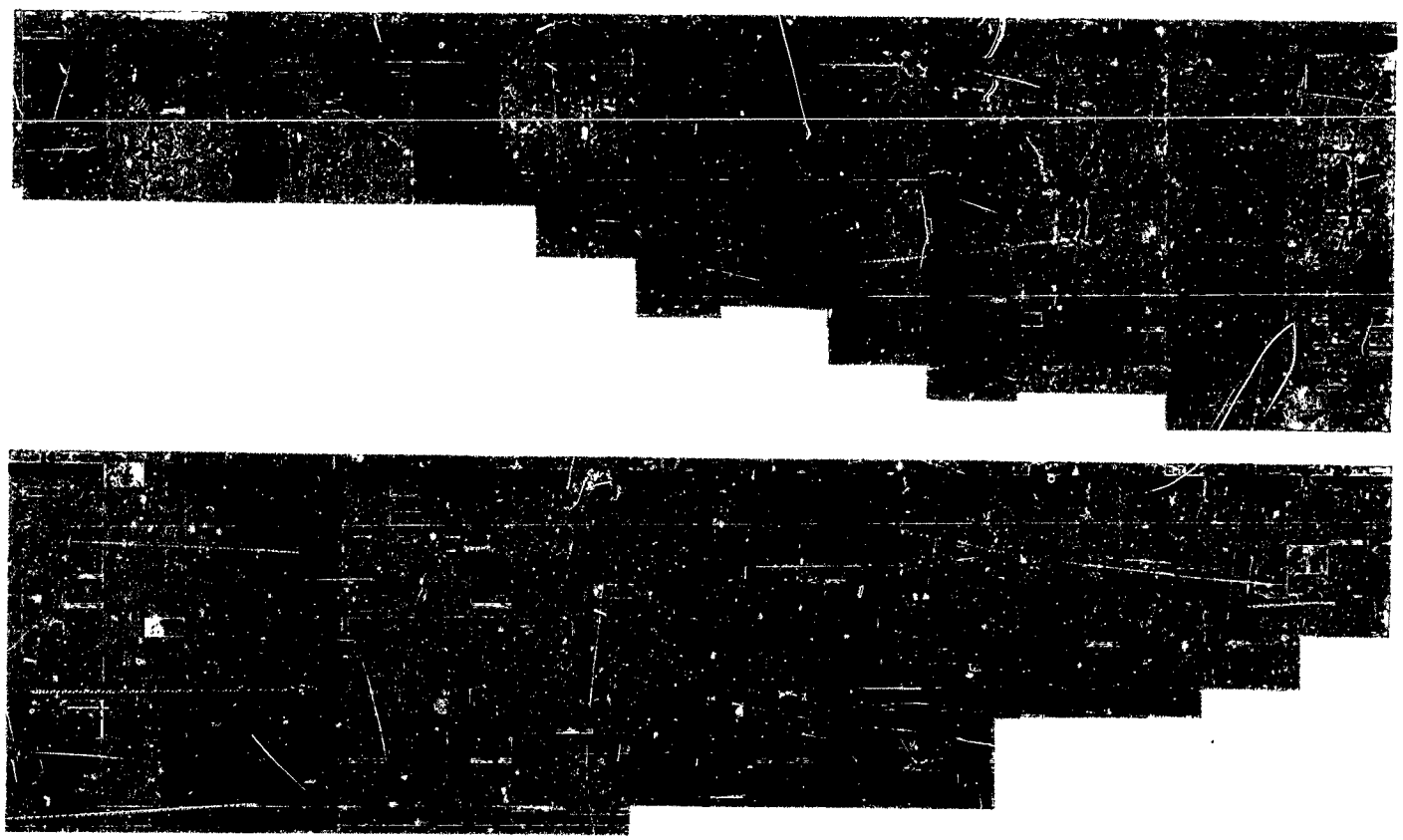

Fig. 9 Cross sections corresponding to numbers in Fig. 8. Definite changes in direction of crack are apparent and are continuous in several adjacent cross sections. A series of these is indicated on several cracks. 350x

Fig. 10 Combination of Figs. 8 and 9 showing third dimension of crack

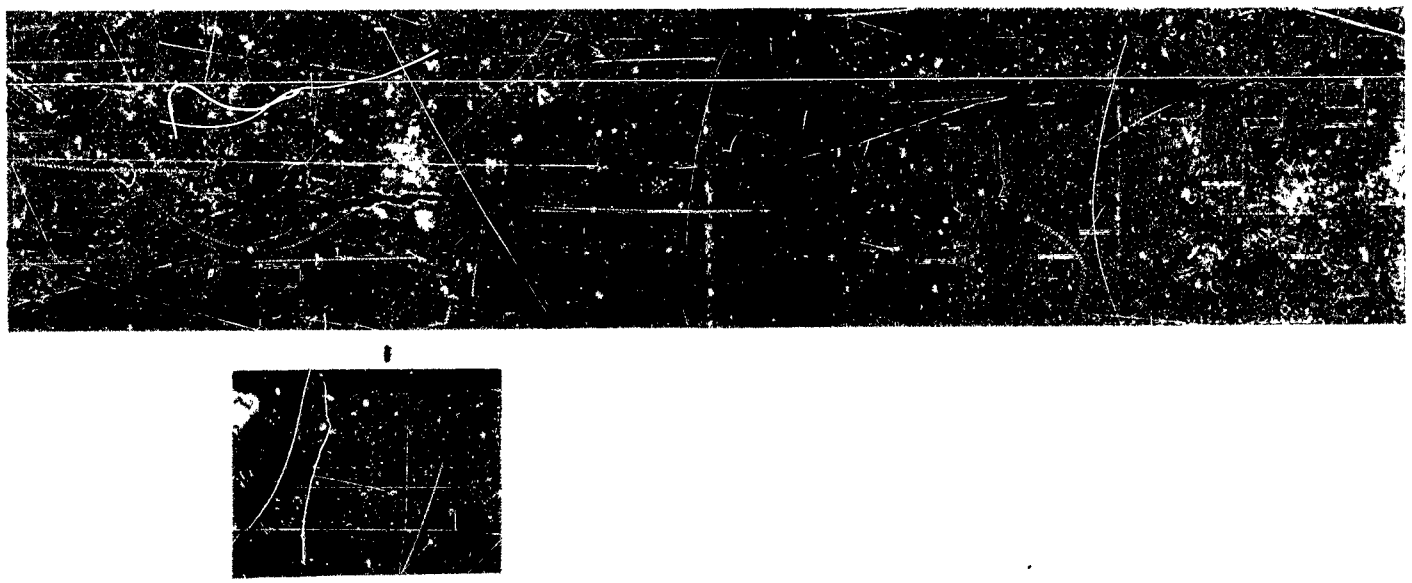

Fig. 11 Surface and one cross section of cracking on abraded surface, suspended in vapor condensation conditions at 400°F over chloride containing waters. Typical cracking pattern at applied stresses above 3,000 psi. 350x

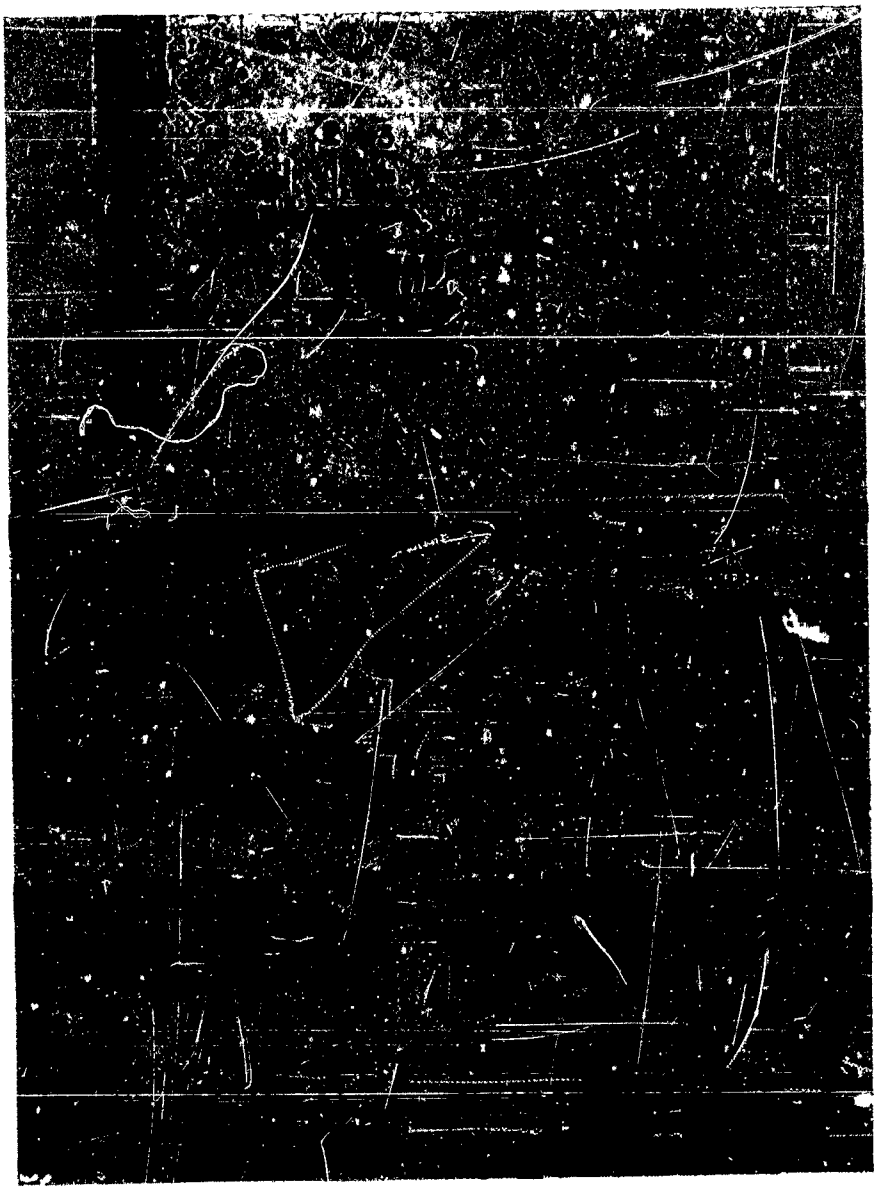

Fig. 12 Surface and associated cross sections of cracking on pickled surface. Solution 875 ppm NaCl, 2,000 psi, held at 400°F for 3 days, vapor condensation conditions. Cross sectional views show the crack proceeding non-perpendicular to the direction of applied stress. 350x

Fig. 13 Inclusions in the crack path. Pickled surface 2,000 psi. Vapor condensation.
(A) Crack arrested. 350x
(B) Crack by-passed. 1370x
(C) Brittle fracture in inclusion. 1370x

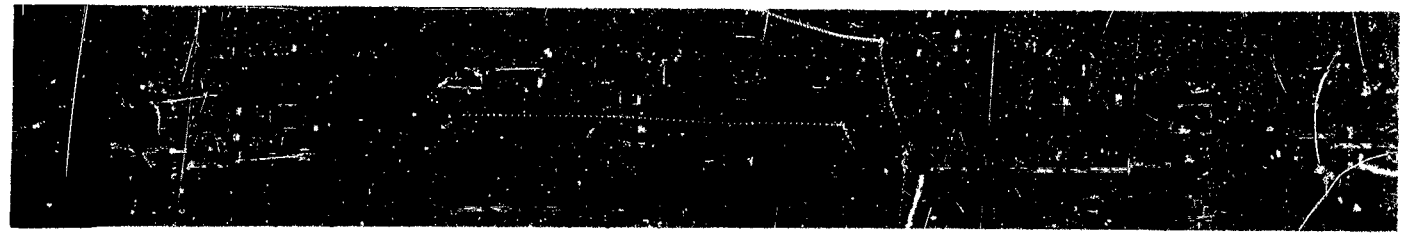

Fig. 14 Surface (Direction A) of crack on specimen immersed for 5 days in 400° water having 20,000 ppm NaCl, stressed to 40,000 psi, and pickled surface. (Numbers refer to corresponding cracks in Fig. 15) 350x

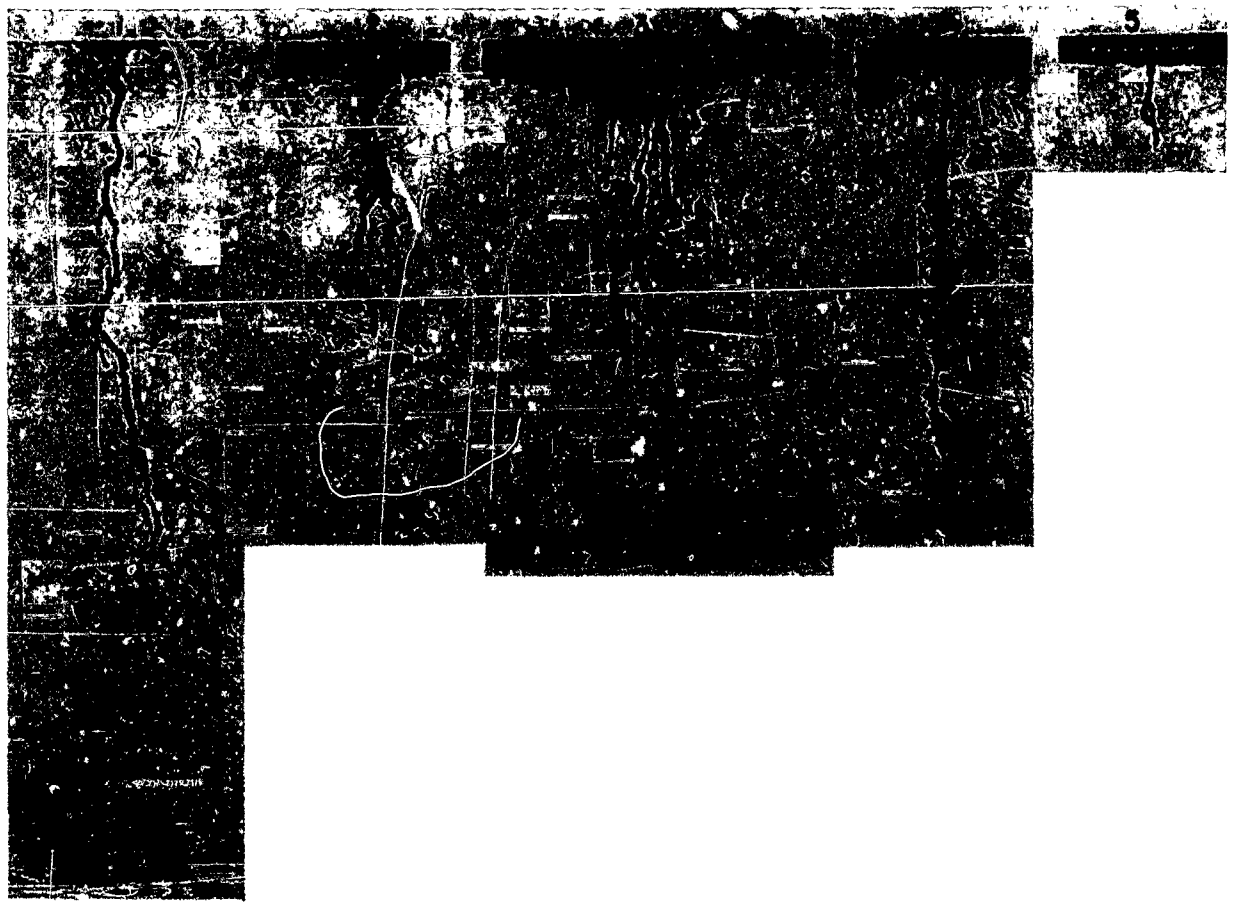

Fig. 15 Cross section of cracks (Direction B) shown in Fig. 14.
350x

Fig. 16 Surface (Direction A) of cracks, abraded surface, applied stress 40,000 psi, immersed in water phase of 20,000 ppm NaCl held at 400°F for five days. (Numbers in brackets refer to particular cracks, numbers not in brackets refer to successive sections.) 350x

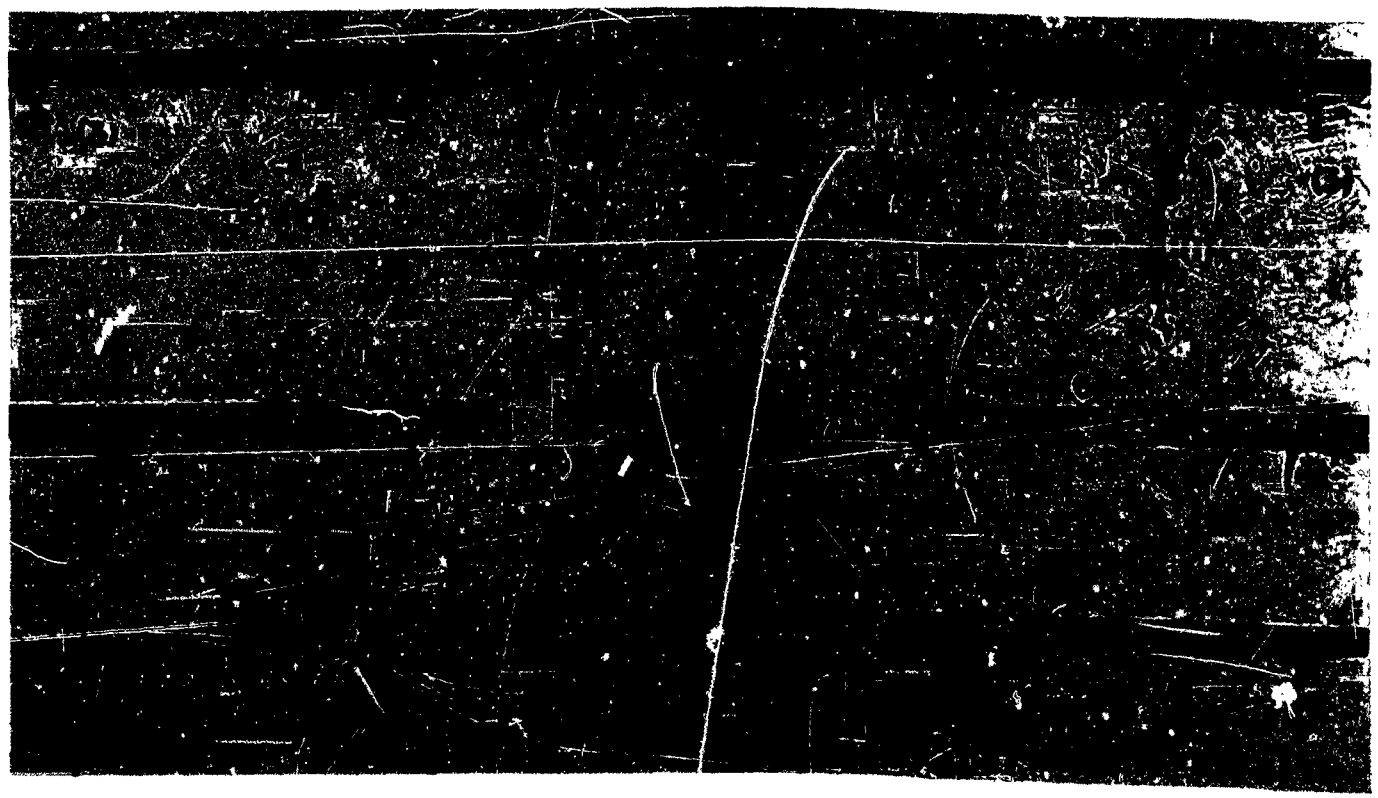

Fig. 17 Cross section of cracks shown in Fig. 16. 350x